

UC Santa Barbara

UC Santa Barbara Electronic Theses and Dissertations

Title

Atypical Protein Kinase C Zeta as a therapeutic target for treatment of Autosomal Dominant Polycystic Kidney Disease

Permalink

<https://escholarship.org/uc/item/3qn2v3m4>

Author

Akbari, Masaw

Publication Date

2020

Peer reviewed|Thesis/dissertation

UNIVERSITY OF CALIFORNIA

Santa Barbara

Atypical Protein Kinase C Zeta as a therapeutic target for treatment of

Autosomal Dominant Polycystic Kidney Disease

A Thesis submitted in partial satisfaction of the
requirements for the degree Master of Arts
in Molecular, Cellular and Developmental Biology

By

Masaw Akbari

Committee in charge

Professor Thomas Weimbs, Chair

Dr. Douglas Thrower

Professor Dzwokai Zach Ma

December 2020

The thesis of Masaw Akbari is approved.

Dr. Douglas Thrower

Dr. Dzwokai Zach Ma

Dr. Thomas Weimbs, Committee Chair

September 2020

PUBLICATION

Akbari M, West JD, Doerr N, Kipp KR, Marhamati N, Vuong S, Wang Y, Rinschen M, Moscat J, Weimbs T. Atypical Protein Kinase C ζ (PKC ζ) is a novel target for treatment of Polycystic Kidney Disease. In preparation.

ABSTRACT

Atypical Protein Kinase C Zeta as a therapeutic target for treatment of Autosomal Dominant Polycystic Kidney Disease

By

Masaw Akbari

Autosomal dominant polycystic kidney disease (ADPKD) is a genetic disorder associated with severe morbidity which affects over 500,000 individuals in the U.S. alone. In most cases ADPKD is caused by a loss-of-function mutation in the *PKD1* gene that encodes polycystin-1 (PC1). While PC1 has been ascribed to regulating numerous signaling pathways that are dysregulated in ADPKD, much of these underlying mechanisms remain to be elucidated.

PC1 has been reported to interact with atypical protein kinase C (aPKC) which is a serine/threonine protein kinase. Data from our lab demonstrates that the zeta isoform of aPKC (PKC ζ) specifically binds to and phosphorylates the C-terminal tail of PC1. PKC ζ also regulates functions which are known to be perturbed in ADPKD such as epithelial cell polarity, ciliogenesis, calcium signaling and metabolism. We thus sought to investigate whether PKC ζ activity is altered in PKD.

We report here that PKC ζ expression is aberrantly downregulated in ADPKD patients as well as in two PKD mouse models. We demonstrate that pharmacologically activating PKC ζ using the FDA approved drug FTY720 ameliorates various markers of disease progression in multiple mouse models. Furthermore, treatment of PKC ζ knockout mice with the drug revealed

reduced efficacy, suggesting a PKC ζ specific mechanism of action. Our data proposes PKC ζ deficiency as a possible driver of PKD and assesses its potential as a drug target in the treatment of ADPKD.

TABLE OF CONTENTS

I. Introduction to Autosomal Dominant Polycystic Kidney Disease.....	7
A. Structure and Function of PC1.....	8
B. Current and Emerging Treatments.....	10
II. Atypical Protein Kinase C ζ is aberrantly expressed in ADPKD and can be targeted pharmacologically to ameliorate disease progression.....	14
III. References.....	40

I. Introduction to Autosomal Dominant Polycystic Kidney Disease

Autosomal Dominant Polycystic Kidney (ADPKD) is the most prevalent genetic kidney disease with an estimated incidence of 1 in 800 live births¹. It is associated with progressively enlarging renal cyst formation that gradually overtakes the normal renal parenchyma and often leads to end-stage kidney disease^{2,3}. ADPKD is the reason for approximately 7 to 10 percent of patients requiring hemodialysis¹. Patients diagnosed with ADPKD also commonly experience flank pain, hypertension, hematuria, polyuria and are susceptible to recurrent urinary tract infections and kidney stones¹.

ADPKD is caused by mutations in *PKD1* encoding polycystin-1 (PC1) or *PKD2* encoding polycystin-2(PC2). Approximately 85% of all ADPKD cases are related to mutations in the *PKD1* gene and mutations in *PKD1* result in a significantly more severe disease relative to mutations in the *PKD2* gene⁴. PC1 and PC2 are known to interact to form a mechanically sensitive cation channel however, numerous other functions have been ascribed to these proteins. Although advances in the field have increased our understanding of the function of PC1, the precise role remains to be elucidated. Additional research is required to better understand how PC1 is regulated which is an important prerequisite for therapy to restore normal polycystin function in patients. Previous work by our group and others have identified Atypical Protein Kinase C (aPKC) as a novel interacting partner of PC1^{5,6}. Specifically, the zeta isozyme (PKC ζ) binds to and phosphorylates PC1⁶. The work here focuses on investigating the potential of PKC ζ to serve as a therapeutic target for treating ADPKD progression.

A. Structure and Function of PC1

The *PKDI* gene encodes PC1 which is a 4293 amino acid protein containing 11 transmembrane domains, a large N-terminal extracellular domain and a short C-terminal cytoplasmic tail^{7,8}. The extracellular portion of PC1 has numerous conserved domains which suggests it may function as a receptor or adhesion molecule^{7,9}. Some examples of these domains include a leucine-rich repeat (LLR), receptor for egg jelly domain (REJ) and a G-protein coupled receptor proteolytic site (GPS)¹⁰. The bulk of PC1 is comprised of the N-terminal domain which is cleaved within the GPS domain and remains noncovalently tethered to the membrane-bound C terminal domain¹¹. The functional role of this cleavage is undetermined but may be a mechanism of stabilizing protein folding.

The C-terminal tail of PC1 is 226 amino acids in length, contains a G-protein activation domain¹², and a coiled-coil motif which is necessary for its interaction with PC2¹³. The C-terminal portion of PC1 can be cleaved releasing fragments which translocate to the nucleus to regulate gene transcription^{14,15}. It has been established that the PC1 tail is phosphorylated by several kinases including PKA¹⁶, Src¹⁶ PRKX¹⁷ and PKC^{5,6}. While the importance of most of these sites require further investigation, functional assays indicate PKC as relevant for proper functioning of PC1^{5,6}.

Data indicates that PC1 and PC2 play an important role in regulating cellular calcium homeostasis. At the base of the primary cilia, PC1 and PC2 interact to function as a mechanically sensitive ion channel that regulates intracellular calcium concentrations¹⁸. The complex responds to bending of the cilium as a result of apical fluid flow¹⁹. Polycystins can also modify calcium release through interaction with other proteins that regulate calcium homeostasis. PC2 and type I inositol 1,4,5-triphosphate receptor (InsP3R) interact to modulate intracellular calcium signaling, while PC1 when localized to the ER binds InsP3R

to decrease the InsP3-induced calcium response²⁰. The 100kDa fragment of the PC1 C-terminal tail also regulate ER calcium stores by binding to the calcium sensor stromal interaction molecule 1 (STIM1) to prevent its translocation to the cell membrane which results in reduced store operated calcium entry²¹.

PC1 and PC2 are also thought to regulate a number of key signaling pathways responsible for diverse cellular functions. Polycystins are proposed to function as regulators of cell-cycle progression^{22,23}, genomic stability²⁴, apoptosis^{25,26}, metabolism²⁷ and cell polarity^{5,28}. These functions may be attributed to the role of the polycystins in modulating mTOR^{29,30}, JAK-STAT^{15,31-34}, AP1^{35,36}, Id2³⁷ and NFAT³⁸ signaling pathways. PC1 is thought to act as a regulator of the mTOR pathway by binding TSC2 to inhibit phosphorylation of tuberin, thus repressing mTOR signaling^{29,40}. A recent study reports that PC1 also acts as a G-protein coupled receptor that binds α subunits³⁹.

PC1 has been implicated in regulating the activity of multiple transcription factors of the STAT family which are frequently found to be activated in various cell types in ADPKD⁴¹. Our group showed that STAT6 activity is inhibited by membrane anchored PC1 yet the cytoplasmic tail fragment can interact with STAT6 and P100 to co-activate STAT6-dependent gene expression¹⁵. Studies from our lab reported a dual mechanism as well as a third mechanism by which PC1 may regulate STAT3. The membrane anchored PC1 can activate STAT3 through JAK-2 dependent phosphorylation or the cleaved 30kDa PC1 C-terminal fragment (PC1-p30) can translocate to the nucleus to co-activate STAT3 (as well as STAT1) which has been activated by cytokine signaling³¹. A third mechanism revealed that PC1-p30 can directly bind to Src to promote phosphorylation and activation of STAT3³³.

It is reported that PC1 and PC2 -either alone or together- are involved in numerous functions yet many of the mechanisms remain to be determined. These same signaling pathways proposed to be regulated by PC1 are also relevant in ADPKD likely as a result of disrupted PC1 signaling. Uncovering the signaling pathways that underlie these functions should facilitate our understanding of ADPKD and lead to development of effective therapeutics.

B. Current and Emerging Treatments

To date there is no cure for ADPKD, first-line treatments focus on preventing end-stage kidney disease (ESKD) by reducing salt intake, controlling blood pressure and managing body weight. For patients who are at high-risk for ESKD the vasopressin 2 receptor antagonist, Tolvaptan, is the only approved drug available. However, adverse effects such as aquaresis and hepatic toxicity compounded by its unfavorable cost restricts the use of this drug⁴². As our understanding of the dysregulated signaling pathways involved in ADPKD expands, other treatment options have been suggested, some of which are currently undergoing clinical trials.

Inhibitors of mTOR have been studied as a potential treatment for ADPKD but none have progressed to approval. mTOR is a protein kinase which phosphorylates downstream targets 4EBP1 and ribosomal protein S6 Kinase resulting in increased cell proliferation. The FDA-approved immunosuppressant Rapamycin was one of the first drugs proposed for treating ADPKD and demonstrated significant decreases in kidney growth in mouse models of PKD^{29,43,44}. TORC1 Inhibitors everolimus and sirolimus also exhibited potent suppression of proliferation in cystic epithelial cells⁴⁵. However, despite successful preclinical studies,

human trials were associated with minimal efficacy due to insufficient drug target delivery and extrarenal side effects. As mTOR signaling plays a critical role in mediating kidney cyst growth innovative approaches to targeted drug delivery might allow mTOR inhibitors to be reconsidered⁴⁶.

The use of re-purposed small molecule drugs have also been studied for treatment of ADPKD, there are currently several under evaluation in clinical trials. Tesevatinib is a novel inhibitor of epidermal growth factor (EGFR) and vascular endothelial growth factor receptor 2 (VEGFR-2) that is presently under investigation for in use in cancer. Tesevatinib has shown efficacy in rodent models of PKD and is currently undergoing phase 2 randomized controlled clinical trials which are expected to be completed in 2022 (ClinicalTrials.gov Identifier: NCT03203642)^{47,48}.

Glycosphingolipids are structural signaling molecules in the cell membrane that regulate aberrant pathways found in ADPKD such as Akt-TORC1 and are found to be accumulated in mouse models of PKD⁴⁹. Using a glucosylceramide synthase inhibitor in *PKDI* conditional knockout mice inhibited cystogenesis suggesting glycosphingolipid metabolism as a potential target for therapy⁵⁰. The orally active glucosylceramide synthase inhibitor, Venglustat re-purposed from trials in Fabry and Gaucher disease is in Phase 2/3 clinical trials in Human ADPKD (ClinicalTrials.gov Identifier: NCT03523728)⁵¹.

Increased Src activity has been linked to ADPKD and pharmacological inhibition in the *pck* rat model resulted in reduced cyst formation⁵². Bosutinib is an oral dual Src/Bcr-Abl tyrosine kinase inhibitor used in the treatment of Philadelphia chromosome-positive chronic myeloid leukemia patients and was found to reduce kidney growth in patients with

ADPKD⁵³. However, the study also reported patients using bosutinib experienced adverse effects such as gastrointestinal and liver toxicity.

There has been significant research recently that aims to target the altered energy metabolism of PKD cyst lining epithelial cells. Cystic cells are reported to have a high rate of glycolysis and low rate of mitochondrial oxidative phosphorylation similar to the Warburg effect in cancer cells²⁷. Research from our lab demonstrated that time-restricted feeding, without caloric reduction strongly inhibited TORC1 signaling, proliferation and fibrosis in experimental models of PKD^{54,55}. This suggests that cystic cells are metabolically inflexible and can be exploited by dietary intervention or supplementation with the ketone beta-hydroxybutyrate (BHB) to induce ketosis⁵⁴. The Warburg effect also results in decreased activity of the energy sensor, adenosine monophosphate activated protein kinase (AMPK), overactivation of cAMP-PKA and ERK, while PI3K/Akt signaling which inhibits the ERK proliferation signaling pathway is inhibited in cystic cells⁵⁶. Metformin is first-line drug for clinical treatment of type 2 diabetes mellitus. Studies report that Metformin acts as a cAMP inhibitor and specifically inhibits mitochondrial respiratory chain complex I and decreases oxidative phosphorylation levels in cells which leads to reduced ATP synthesis, activating AMPK and inhibiting mTOR proliferation signaling pathway⁵⁷⁻⁵⁹. Preclinical studies of Metformin have shown effectiveness in slowing progress of PKD and there are presently two safety and tolerability clinical trials in progress⁶⁰⁻⁶². Recently, the effects of a combination therapy using Metformin and 2-deoxyglucose (2-DG) was investigated on cell proliferation, apoptosis and glucose metabolism of renal cystic epithelial cells⁶³. The results indicated a low-dose combinational use of both drugs inhibited proliferation and increased apoptosis, while lowering intracellular ATP levels in cystic cells.

STAT overactivation is frequently observed in multiple cell types in ADPKD and PKD animal models which suggests it may act as a driver of disease progression. STAT3 inhibition has been intensely studied in the cancer field because of its involvement in cancer cell transformation, apoptosis and proliferation⁶⁴. These effects are being tested in PKD and there are a number of inhibitors being investigated⁶⁵. For instance, compounds that inhibit STAT3 dimerization have been shown to reduce disease progression in PKD⁶⁶. The natural compound curcumin was shown to strongly inhibit STAT3 in *PKDI* deletion mice and is currently undergoing clinical trials for the treatment of ADPKD (ClinicalTrials.gov Identifier: NCT02494141)⁶⁷. Our lab has shown that STAT6 is aberrantly activated in cyst lining epithelial cells in PKD and pharmacological inhibition of STAT6 using the immunosuppressant teriflunomide leads to inhibition of cyst growth³². Research reveals direct connections between PC1 and STAT signaling which underlines the importance of identifying a therapeutic approach to target the overactivation of STAT signaling.

II. Atypical Protein Kinase C is aberrantly expressed in ADPKD and can be targeted pharmacologically to ameliorate disease progression

Introduction

Autosomal dominant polycystic kidney disease (ADPKD) is the most common genetic kidney disease, affecting over 12 million people worldwide. The cause is linked to mutations in either the *PKD1* or *PKD2* gene. Disease progression involves the formation of numerous fluid filled cysts throughout both kidneys that progressively enlarge, replacing the normal renal parenchyma and eventually causing end stage renal disease in most ADPKD patients prior to the sixth decade^{4,68}. ADPKD is a disease for which there remains an overwhelming need for treatment. Currently, Tolvaptan is the only FDA approved drug for the treatment of symptoms, however patient access to Tolvaptan is limited due to its extremely high cost and severe extra renal side effects. Most ADPKD patients will eventually require renal transplantation or dialysis.

The *PKD1* gene encodes polycystin-1 (PC1), an approximately 500 kDa glycoprotein comprised of a large extracellular domain, 11 transmembrane domains, and a short cytoplasmic tail⁶⁸. The *PKD2* gene encodes polycystin-2 (PC2), a 130 kDa non-selective cation channel of the TRP family⁶⁹. PC1 and PC2 interact via their coiled-coil motifs in their C-terminal tails and are thought to form a mechanically sensitive, cation channel. However, numerous other functions have been ascribed to these proteins, and the actual purpose of the polycystins is not well understood⁶⁸. PC1 has been shown to localize to several cellular compartments including primary cilia, cell-cell junctions, the endoplasmic reticulum and the nucleus⁷⁰⁻⁷³. PC1's diversity of subcellular localizations supports its involvement in many

complex intracellular signaling pathways. Within the PC1 sequence, most of the reported protein interactions map to its ~200 residue C-terminal cytoplasmic tail.

Our lab and others have shown PC1 regulates STAT3 and mTOR signaling^{29,41,74}, both of which are vastly dysregulated in human ADPKD and rodent models of PKD. STAT3 is shown to be strongly activated in cyst-lining epithelial cells in human ADPKD³¹ and in several PKD rodent models^{31,54,66,67,75}, compared to normal kidneys. Initial inhibitor studies suggest that aberrant STAT3 activation may be a driving force of renal cyst growth^{66,67,76}, however these inhibitors express limited specificity and off-target effects. Besides STAT3 signaling, numerous other aberrantly activated signaling pathways have been associated with renal cyst growth including the mammalian target of Rapamycin (mTOR). Unfortunately, inhibitors of mTOR have had little success in clinical trials due to the dose-limiting toxic effects.

The PC1 C-terminal tail interacts with several kinases *in vitro* including PKA¹⁷, PRKX¹⁷, and Src⁷⁷. We have previously shown the tyrosine kinase, JAK2, interacts with the membrane-proximal portion of the PC1 tail and regulates PC1-dependent STAT3 activation³¹. Work from our lab indicates that atypical protein kinase C (aPKC), specifically the zeta isozyme, can bind to and phosphorylate the C-terminal tail of PC1⁶. Furthermore, Castelli et al. have demonstrated a functional interaction between PC1 and aPKC to mediate polarized cell migration during embryonic renal development⁵. They report that directional cell division is disrupted in mouse models of PKD due to dysregulation of the Par3/6 polarity complexes. However, regulation and expression at the level of PKC ζ activity were not fully explored.

The atypical protein kinase C family (aPKC), which includes isoforms ζ (PKC ζ) and λ (PKC λ), require neither calcium nor DAG for activation⁷⁸. PKC ζ is well known for its role in epithelial cell polarity, ciliogenesis, metabolism, calcium signaling, as well as in various signaling pathways which are also disrupted in ADPKD, including NF- κ B^{79,80}, AMPK⁸¹ and S6K⁸²⁻⁸⁵.

In this present study we investigate the activity of PKC ζ in PKD and report that PKC ζ levels are reduced in both human ADPKD and PKD mouse models. We provide evidence that pharmacological activation of the protein via treatment with the FDA-approved drug fingolimod (FTY720) can significantly reduce STAT3 overactivation, cell proliferation and cyst growth in PKD mouse models. Taken together, these results indicate that PKC ζ plays a critical role in the pathogenesis of ADPKD and suggests that PKC ζ is not only dysregulated in the disease, but also contributes to aberrant epithelial cell proliferation and renal cyst growth. Furthermore, these data reveal that aberrant PKC ζ activity can be pharmacologically targeted to alleviate disease burden, thus providing a novel therapeutic approach to ADPKD.

Results

The results described here includes contributions from N. Doerr and J. West.

PKC ζ expression is downregulated in the kidneys of ADPKD patients and PKD mouse models

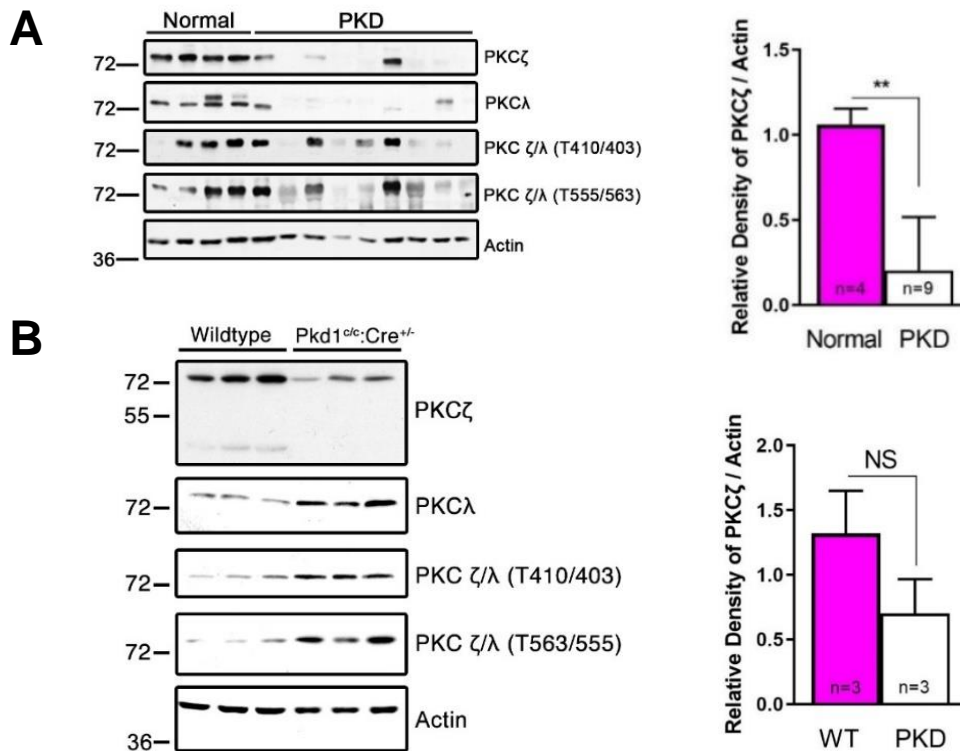
Our lab as well as others have confirmed that PC1 and PKC ζ interact^{5,6} and that PKC ζ phosphorylates PC1⁶. We next wanted to better understand how PKC ζ signaling is altered in PKD. By western blot analysis, we observed decreased levels of PKC ζ in kidney tissue

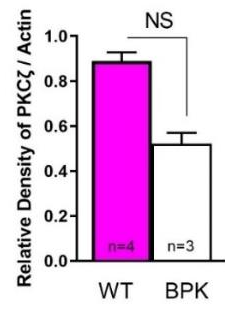
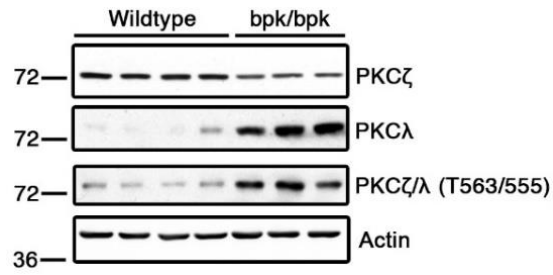
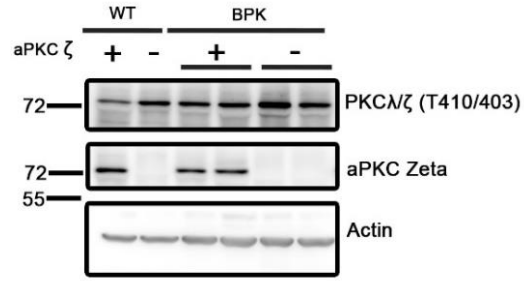
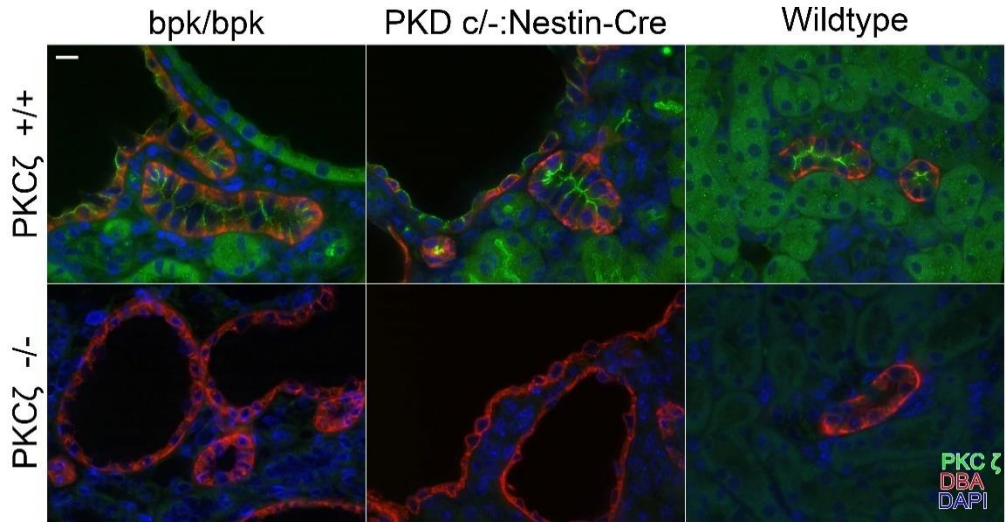
lysates from human ADPKD patients (Fig. 1A), as well as, kidney tissue lysates from the ADPKD orthologous $Pkd1^{cond/cond};Nes^{Cre}$ ($Pkd^{cond/cond}$) (Fig. 1B) and non-orthologous bpk mouse models (Fig. 1C), as compared to control mice. The atypical PKC (aPKC) family consists of two closely related proteins, PKC ζ and λ . Unexpectedly, we noticed an increase in total phosphorylated aPKC (PKC ζ/λ) at both the T555/563 and T410/403 sites in multiple mouse models using antibodies that cannot distinguish between these two aPKC forms (Fig. 1B, 1C). Phosphorylation at these sites indicates activation of aPKC. Given that we found PKC ζ to be downregulated but observed increased PKC λ expression (Fig. 1B, 1C), we attributed the increase in apparent aPKC phosphorylation to upregulated PKC λ . In fact, analysis of both wildtype and bpk mice with a transgenic knockout of PKC ζ expressed minimal changes in phosphorylation of total aPKC when compared to unaltered mice (Fig. 1D). This suggests a compensatory mechanism between the two aPKC isoforms in mouse models. When we assessed aPKC expression changes in human ADPKD patients, we failed to see a similar up-regulation of PKC λ and therefore, did not investigate these changes further.

To explore the localization of PKC ζ *in vivo*, we employed immunofluorescence microscopy on kidney sections. In kidneys of wild-type mice, PKC ζ localizes diffusely in the cytoplasm of tubule cells except in collecting duct/ distal tubule cells where it localizes very distinctly to apical junctions (Fig. 1E). Kidneys from PKC ζ null mice were used as negative controls to ensure specificity of the immune signal. Renal collecting duct marker Dolichos Biflorus Agglutinin (DBA) revealed that PKC ζ localizes most frequently to the apical junctions of distal tubule epithelial cells in both wild-type and cystic mouse kidneys

(*Pkd1*^{cond/-} and *bpk* mouse models) (Fig. 1E). This is consistent with the cellular origin of the these cysts which are primarily derived from collecting duct/ distal tubule cells⁴³. Because PKC ζ expression was reduced in human patients and PKD mouse models (Fig 1A-C) yet the localization was similar between wildtype and cystic mouse kidneys (Fig. 1E), we hypothesized that PKC ζ dysregulation in PKD is a factor of impaired expression rather than mis-localization.

Figure 1 PKC ζ expression is dysregulated in PKD. (A) Western blots of kidney tissue lysates from normal or ADPKD patients and relative density normalized to actin. (B) Western blots of kidney tissue lysates from post-natal day 49 *Pkd1*^{cond/cond} or wildtype mice and relative density normalized to actin. (C) Western blots of kidney tissue lysates from post-natal day 17 *bpk/bpk* or wildtype mice and relative density normalized to actin. Blots completed by ND. (D) Western blot of kidney tissue lysates from *bpk* or wildtype mice that have a transgenic knockout of PKC ζ . (E) Immunofluorescence staining of PKC ζ (green), DBA marker of renal collecting ducts (red) and nuclei (blue) 5 μ M kidney sections from cystic (*bpk/bpk*, PKD *c/-:Nestin-Cre*) and wildtype (WT) mice. Scale bar =10 μ M

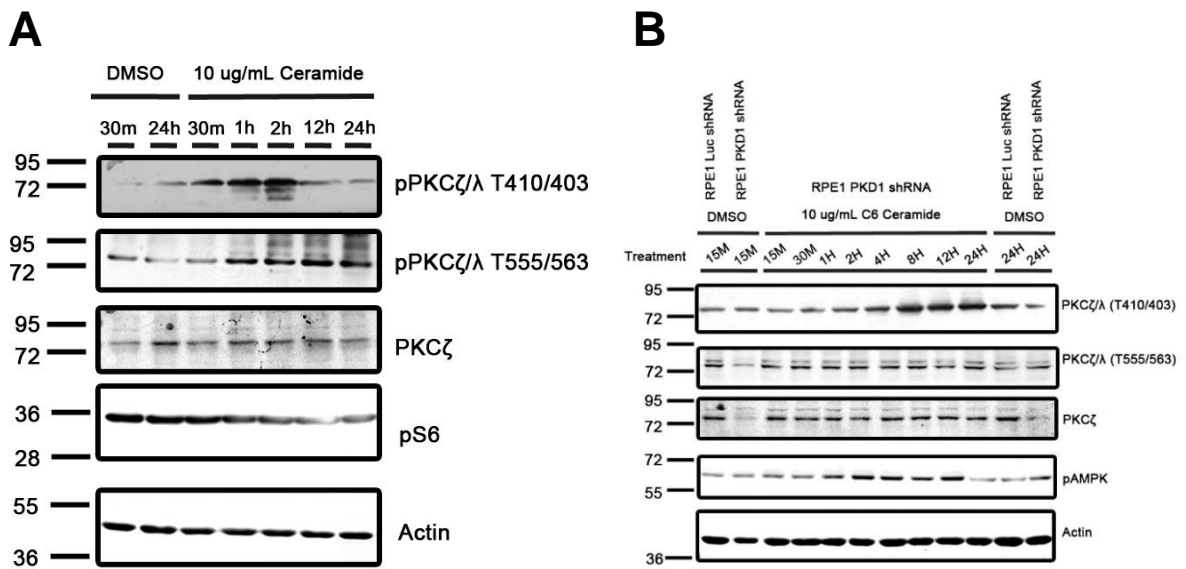


C**D****E**

Ceramide activates PKC ζ in *in vitro* models of PKD

Given our findings that PKC ζ is dysregulated in PKD and that a PKC ζ knockout has no accelerating effect on the disease in the two tested mouse models, we hypothesized that restoring PKC ζ activity and expression in PKD may slow disease progression. C6 Ceramide is a non-physiological sphingolipid that is well known to specifically activate the PKC ζ isoform^{86,87,88}, as well as, inhibit mTOR activity^{89,90}. Consistent with these findings, we found that treatment of IMCD cells with 10 $\mu\text{g/ml}$ of C6 Ceramide activated PKC ζ (pThr⁴¹⁰) and slightly inhibited S6 in a time-dependent manner (Fig. 2A). We next sought to assess the potential effect of C6 Ceramide in an *in vitro* model of PKD, where PKC ζ expression is altered. To achieve this, we used retinal pigment epithelial (RPE1) cells with a stably integrated Pkd1 shRNA knockdown (PKD1 shRNA) (Fig. 2B). Treatment of these PKD1 shRNA RPE1 cells with 10 $\mu\text{g/ml}$ of C6 Ceramide demonstrated activation of PKC ζ as well as downstream AMPK from 8 hours to at least 24 hours post-treatment (Fig. 2A). These findings suggested that C6 Ceramide has the capability to activate PKC ζ in the context of PKD and supported proceeding to treatment of mouse models with the sphingolipid. However, due to its poor bioavailability, the formation of nanoliposomes is required to inject the lipid *in vivo*^{91–93}. Given this limitation, we aimed to stabilize PKC ζ activity pharmacologically using FTY720 (Fingolimod/Gilenya, Novartis), a first-in-class small molecule immunomodulatory drug approved by the FDA for use in relapsing multiple sclerosis⁹⁴.

Figure 2 Ceramide activates PKC ζ *in vitro* (A) IMCD cells treated with DMSO or Ceramide for 30 minutes, 1 hour, 2 hours, 12 hours or 24 hours showed activation of PKC zeta and slight inhibition of pS6. (B) Western bot of RPE1 cells with a stable shRNA knockdown of either Pkd1 (Pkd1 shRNA) or scramble control (Luc shRNA), treated with 10 ug/mL of C6 Ceramide over a time course treatment. Completed by JW.



FTY720 activates PKC ζ *in vitro* and *in vivo* models of PKD

FTY720 is a sphingosine 1-phosphate analog derived from myriocin and a substrate of sphingosine kinase. Importantly, FTY720 has been shown to upregulate endogenous ceramide levels⁹⁵, which suggested that the drug could indirectly activate PKC ζ and restore its function in PKD. Additionally, the drug has been shown to inhibit the signaling of the Akt/mTOR axis⁹⁶, STAT3⁹⁷, HDACs⁹⁸ and HIF1 α ⁹⁹, all of which are aberrantly increased in PKD mouse models and human ADPKD. Taken together, these considerations suggest that FTY720 treatment may improve PKD progression.

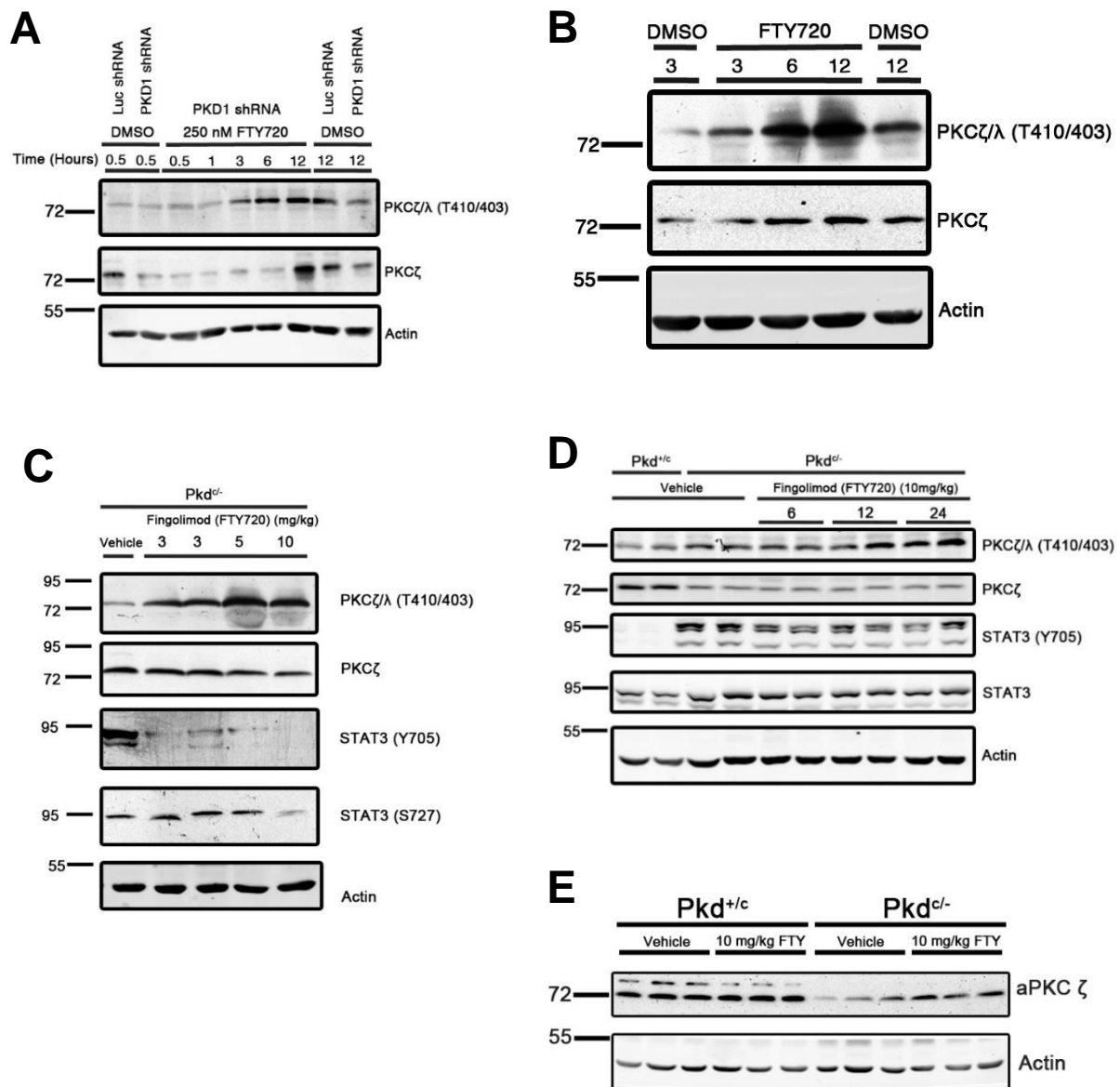
Before injecting FTY720 *in vivo*, we sought to confirm that the drug can activate PKC ζ in our *in vitro* model of PKD. We treated PKD1 shRNA RPE1 cells with 250 nM FTY720 over a time course and found that PKC ζ was not only activated at multiple time points, but also that its expression was stabilized after 12 hours of treatment, compared to vehicle controls in PKD1 shRNA and luciferase shRNA (Luc shRNA) control cells (Fig. 3A). Importantly, the expression of PKC ζ after 12 hours of FTY720 treatment mimicked the expression level in the vehicle treated Luc shRNA cells, suggesting that the drug has the potential to not only activate PKC ζ in the context of PKD, but also return its expression to baseline levels. We also treated MDCK cells with 1 μ M FTY720 over a time course and found that PKC ζ was indeed robustly activated, most significantly at 12 hours, as compared to vehicle controls (Fig. 3B).

We next investigated the effects of FTY720 in an orthologous mouse model of ADPKD in which the *Pkd1* gene is conditionally inactivated by Cre recombinase driven by the nestin promoter $Pkd1^{cond/-};Nes^{Cre}$ ($Pkd^{cond/-}$). First, we assessed dose-dependent signaling changes by injecting 3, 5 or 10 mg/kg FTY720, euthanizing the mice 12 hours later and analyzing the renal tissue lysates by western blot (Fig. 3C). As predicted, we observed strong activation of PKC ζ

with all 3 doses, compared to vehicle controls. However, we did not observe any change in the total PKC ζ expression in the Pkd1^{cond/-} mice kidneys. We also observed inhibition of phospho-STAT3 (Y705) in all 3 doses as well as less significant inhibition at Serine 727, most notably with the 10 mg/kg dose.

Additionally, we monitored time-dependent signaling changes at 6, 12 and 24 hours after a single injection of 10 mg/kg FTY720 (Fig. 3D). Consistent with our prior results, PKC ζ was activated, at 12 and 24 hours. Similar to the dose response single injection experiment, the expression of total PKC ζ was unchanged at all 3 time points. *In vitro* treatment with FTY720 resulted in stabilized PKC ζ expression and activation, while single injection *in vivo* treatment exhibited PKC ζ activation alone. Analysis of daily *in vivo* FTY720 injections spanning from post-natal day 7 to 20 showed activation of PKC ζ compared to vehicle (Fig. 3E). This leads us to conclude that the differences may be due to the pharmacokinetics of FTY720. Additionally, phosphorylation of STAT3 (Y705) appeared inhibited (Fig. 3D), consistent with the dose response injection results (Fig. 3C). Overall, the results of *in vitro* and *in vivo* studies indicated that FTY720 can activate PKC ζ , and inhibit STAT3, both of which are dysregulated in PKD.

Figure 3 FTY720 activates PKC ζ *in vitro* and *in vivo* (A) Western blot of RPE1 cells with a stable shRNA knockdown of either Pkd1 (Pkd1 shRNA) or scramble control (Luc shRNA), treated with 250 nM FTY720 over a time course. Completed by JW. (B) Western blot of MDCK cells treated with 1 μ M FTY720 or DMSO control over a time course of 3, 6 or 12 hours. (C) Western blot of kidney tissue lysates from cystic (Pkd1^{cond/-}) mice injected with a single dose of 3, 5 or 10 mg/kg FTY720, compared to vehicle controls. Mice were euthanized 12 hours after IP injection. (D) Immunoblot of kidney tissue lysates from cystic (Pkd1^{cond/-}) mice injected with a single dose of 10 mg/kg FTY720 and euthanized at 6, 12 or 24 hours after IP injection. Cystic and wildtype (Pkd1^{+c}) vehicle controls are included. Completed by JW. (E) Cystic and wildtype PKD mice treated with daily IP injections of 10 mg/kg FTY720 or vehicle from post-natal day 7 to 20 tissue was harvested 12 hours after the last injection and kidney lysates were analyzed by western blot.



FTY720 improves disease progression in multiple mouse models of PKD in a PKC ζ dependent manner

Given these promising initial findings, we proceeded to treat the ADPKD orthologous Pkd1^{cond/-} mouse model with daily intraperitoneal (IP) injections of 10 mg/kg FTY720 from post-natal day 7 to 20 and found that this treatment improved disease progression. This finding is shown by representative gross kidney images, representative H&E stained full kidney sections (Fig. 4A), and cystic index (Fig. 4C) comparing wildtype (PKD^{+c}) and cystic (PKD^{c/-}) mice that are wildtype for PKC ζ (PKC ζ +/+). These results are supported by significant reduction in the two-kidney to body weight coupled with a non-significant trend towards decreased BUN of treated cystic mice, as compared to vehicle control (Fig. 4B).

Kidney interstitial fibrosis is a hallmark of PKD, we therefore investigated the effect of FTY720 on collagen deposition. It was found that FTY720 attenuates fibrosis in cystic mice as shown by the Sirius Red stain (Fig. 4D). We also investigated the accumulation of myofibroblasts which are known to contribute to the production of extracellular matrix proteins such collagen I and collagen III, promoting interstitial fibrosis^{100,101}. In agreement with the decrease in collagen deposition, FTY720 markedly decreased the presence of myofibroblasts as shown by immune-staining for alpha-smooth muscle actin (Fig. 4E). We also probed for the accumulation of macrophages which has been shown to contribute to PKD progression¹⁰²⁻¹⁰⁵. Our studies indicated that FTY720 treatment of PKD kidneys significantly reduced the macrophage marker F4/80 in cystic kidneys (Fig. 4F). TUNEL assay and immunofluorescence staining for cell cycle marker Ki-67 revealed FTY720 suppresses apoptosis and proliferation respectively (Fig. 4G, 4H), both of which are increased in PKD.

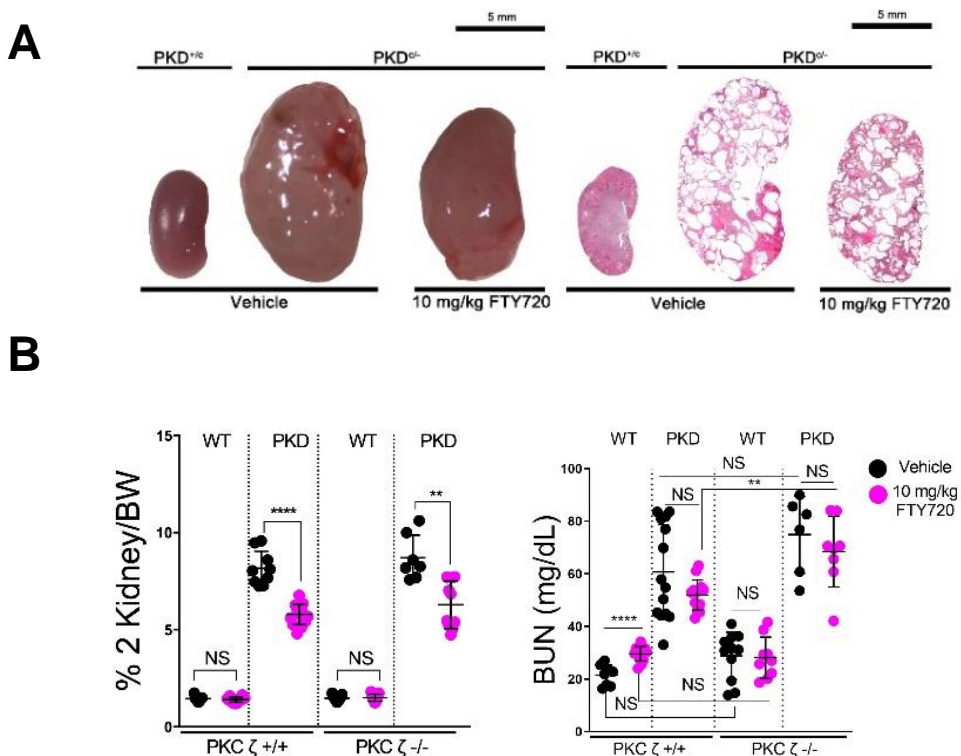
We also treated the non-orthologous bpk polycystic kidney mouse model with daily 10 mg/kg IP injections of FTY720 from post-natal day 7 to 16 and found similar attenuation of cyst progression as seen in treatment of the $Pkd1^{cond/-}$ model. Gross kidney analysis and H&E staining demonstrated that cystic (bpk/bpk) mice treated with FTY720 produced significant decreases in kidney size (Fig. 5A), two kidney to body weight (Fig. 5B), BUN (Fig. 5B), cystic index (Fig. 5C) and fibrosis (Fig. 5D). Likewise, bpk kidneys exhibited decreases in alpha-smooth muscle actin, macrophages, apoptosis, and proliferation (Fig. 5E-H).

Importantly, we found that improvement in PKD progression with FTY720 treatment was specific to PKC ζ . When comparing markers of disease progression between PKC ζ $+/+$ and PKC ζ $-/-$ mice treated with FTY720, PKC ζ $+/+$ mice experienced greater benefit than PKC ζ $-/-$ mice. This was most prominently demonstrated when comparing STAT3 activity in treated cystic kidneys of PKC ζ $+/+$ mice to PKC ζ $-/-$ mice. STAT3 has previously been reported to be activated in PKD and drives cyst progression^{31,33,41,66,67,75}. The drug treatment significantly reduced STAT3 activity in $Pkd1^{cond/-}$ and bpk mice but had minimal effect on PKC ζ $-/-$ mice (Fig. 4I, 5I). These findings indicate that FTY720 mediated STAT3 inhibition is likely dependent on PKC ζ activity. Furthermore, decreases in proliferation marker Ki-67, cystic index and apoptosis appear to also be PKC ζ dependent effects. The decreases in two-kidney to body weight and fibrosis appear to be less PKC ζ specific. These effects can be attributed to the known anti-fibrotic action of the drug¹⁰⁶⁻¹⁰⁸.

These results suggest that the FDA-approved drug FTY720 ameliorates disease progression in PKD mouse models and does so through a novel mechanism of action. We have shown that the beneficial effects of FTY720 are in part related to the activity of PKC ζ , which

we found is aberrantly downregulated in PKD. Our studies introduce PKC ζ as a promising therapeutic target for treatment of ADPKD.

Figure 4 FTY720 improves disease progression in the ADPKD orthologous Pkd1^{cond/-} mouse model while improvement is diminished in PKC ζ knockout mice. Wildtype, cystic PKD (Pkd^{cond/-}) and wildtype, cystic PKD crossed into PKC ζ null mice were treated with daily intraperitoneal (IP) injections of 10 mg/kg FTY720 or vehicle control from day 7-20 and assessed for disease progression. **(A)** Representative gross kidney images of wild-type and PKD vehicle or FTY720 treated (left) and representative 4X images of full kidney H&E stained kidney sections (right) **(B)** two-kidney to body weight (% 2K/BW) (left) and blood urea nitrogen (right) **(C)** Representative images of H&E stained wildtype, PKD and PKD PKC ζ null mouse kidneys (left) and percent cystic index (right), **(D)** Sirius red fast green collagen staining of PKD mouse kidneys (left) and percent fibrosis (right). Immunofluorescence of PKD or PKD PKC ζ knockout mice kidneys treated with 10 mg/kg FTY720 or Vehicle injection and quantification of alpha-smooth muscle actin **(E)** and macrophage marker F4/80 **(F)**. **(G)** TUNEL assay for apoptosis of PKD and PKD PKC ζ null kidney sections and percent of TUNEL positive cells. **(H)** Ki-67 cellular proliferation marker immunofluorescence stain and quantification performed by counting the cyst lining positive Ki-67 cells per total cyst lining cells. **(I)** Immunohistochemical stain for phospho-STAT3 (Y705) of PKD and PKD PKC ζ null kidney sections and quantification. The scale bars =50 μ M.



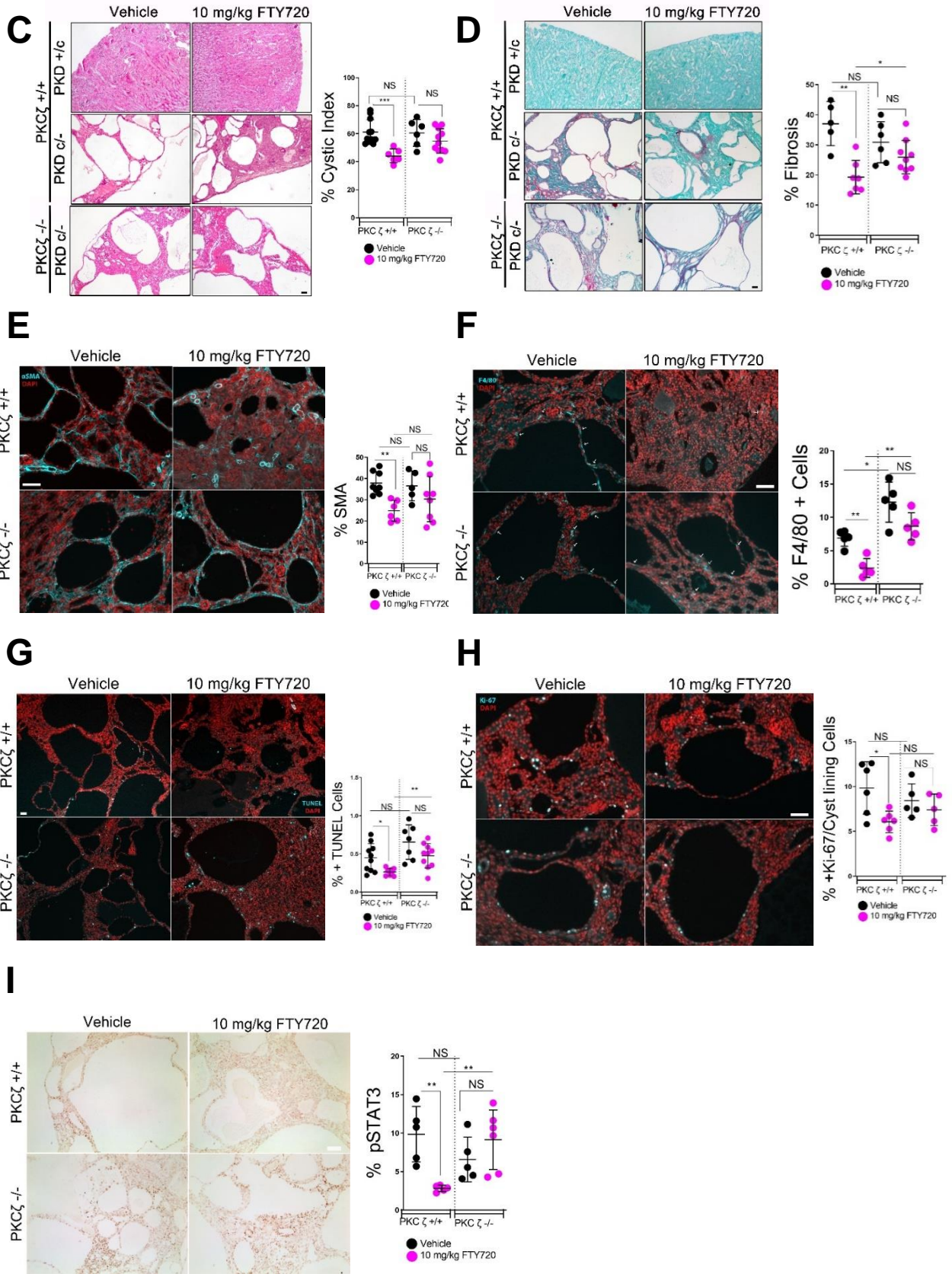
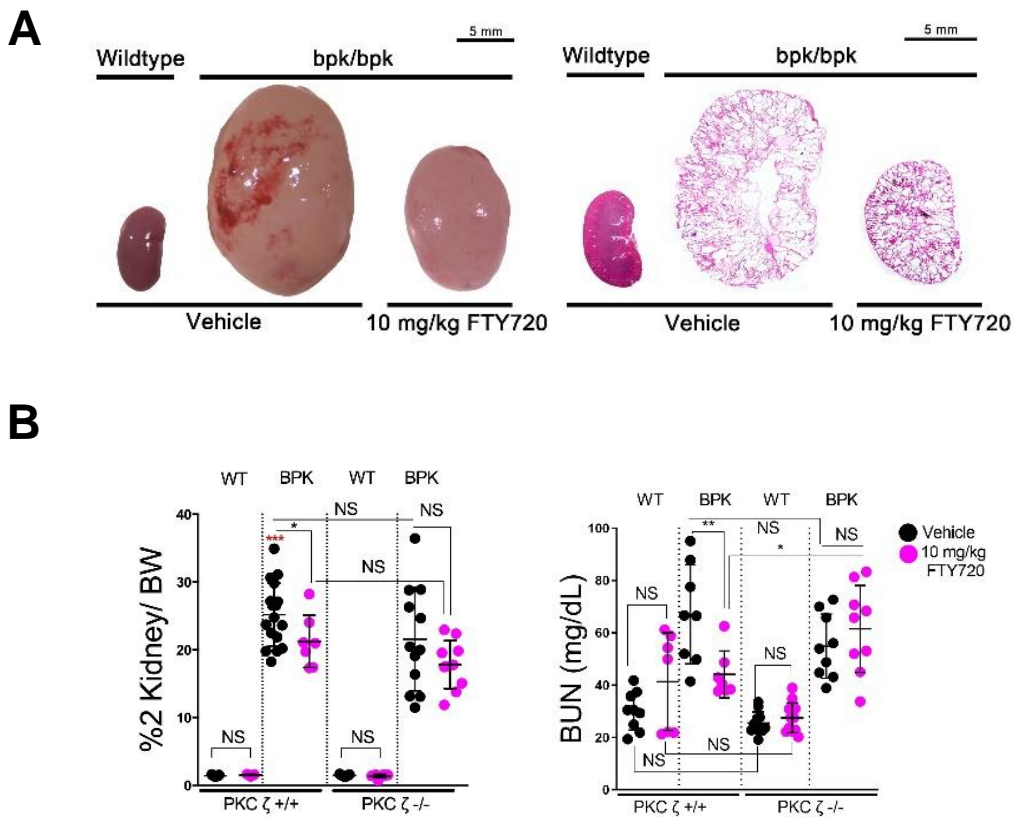
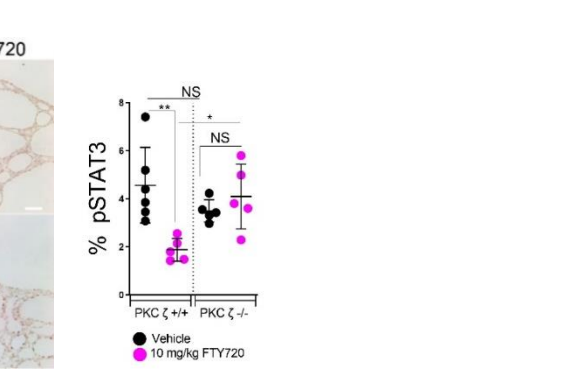
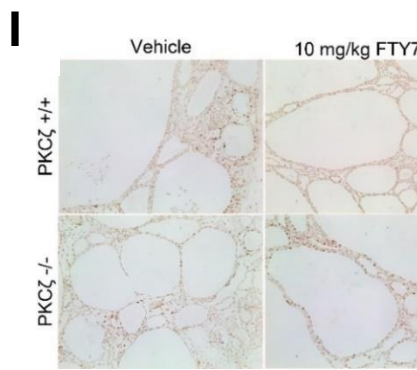
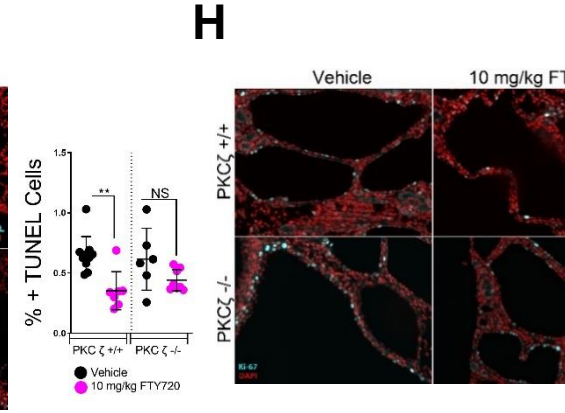
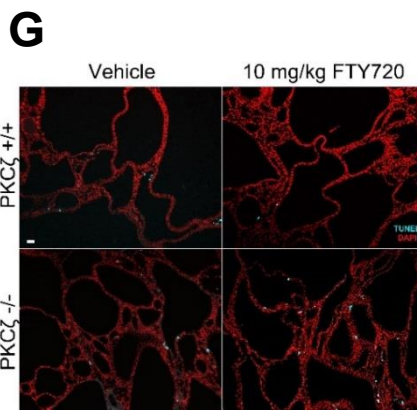
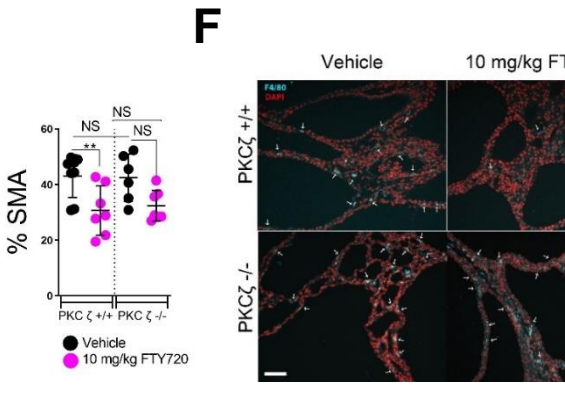
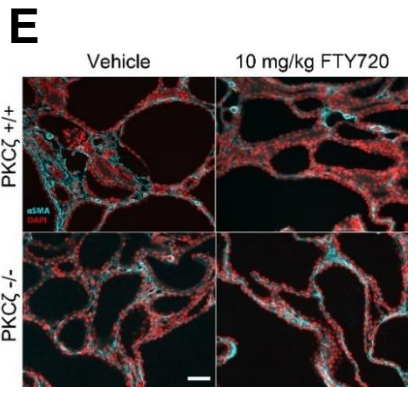
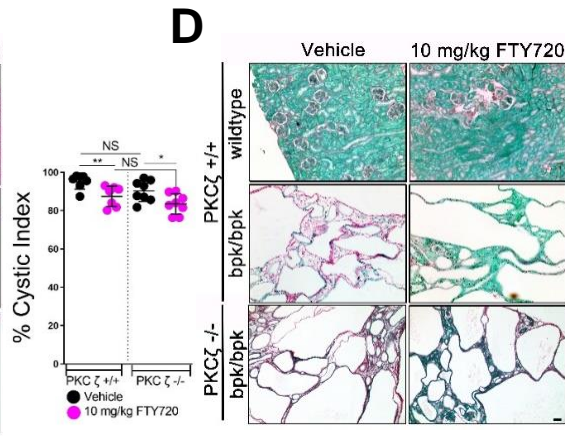
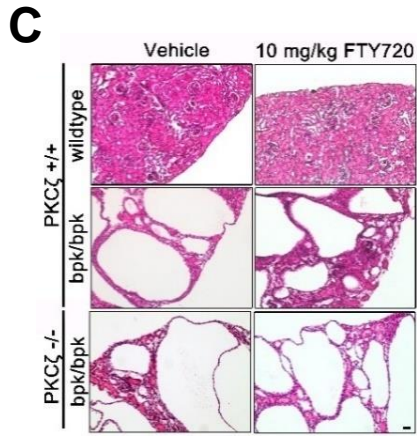


Figure 5. FTY720 improves disease progression in the BPK mouse model while the improvement is diminished in BPK PKC ζ knockout mice. FTY720 improves disease progression in the BPK mouse model, while the improvement is diminished in BPK PKC ζ knockout mice. Wildtype and cystic mice were treated with daily intraperitoneal (IP) injections of 10 mg/kg FTY720 or Vehicle control (2% DMSO) from day 7-16 and assessed for disease progression. **(A)** Representative gross kidney images of wild-type and BPK vehicle or FTY720 treated (left) and representative 4X images of full kidney H&E stained kidney sections (right) **(B)** two-kidney to body weight (% 2K/BW) (left) and blood urea nitrogen (right) red asterisk represents end stage renal failure **(C)** Representative images of H&E stained wildtype, BPK (bpk/bpk) and BPK PKC ζ null mouse kidneys (left) and percent cystic index (right) **(D)** Sirius red fast green collagen staining of BPK mouse kidneys and percent fibrosis. Immunofluorescence of BPK or BPK PKC ζ knockout mice kidneys treated with 10 mg/kg FTY720 or Vehicle injection and quantification of alpha-smooth muscle actin **(E)** and macrophage marker F4/80 **(F)**. **(G)** TUNEL assay for apoptosis of BPK and BPK PKC ζ null kidney sections and percent of TUNEL positive cells. **(H)** Ki-67 cellular proliferation marker immunofluorescence stain and quantification performed by counting the cyst lining positive Ki-67 cells per total cyst lining cells. **(I)** Immunohistochemical stain for phospho-STAT3 (Y705) of BPK and BPK PKC ζ null kidney sections and quantification. The scale bars =50 μ M.





Discussion

In this study, we demonstrate that PKC ζ is aberrantly expressed in ADPKD and that PKC ζ expression can be pharmacologically modulated in both *in vitro* and *in vivo* models of PKD. Furthermore, we show PKC ζ downregulation is at least a partial driver of renal cyst growth because pharmacological activation of PKC ζ using FTY720 significantly ameliorates the disease in PKD mouse kidneys expressing PKC ζ , more so than in PKC ζ knockout kidneys. We have identified PKC ζ as a novel driver of PKD cyst progression which can be pharmacologically targeted as a potential strategy in treating ADPKD.

The mechanism by which PKC ζ levels are being decreased in PKD remains unclear and a subject of future investigation. It has been reported that fluid flow protects PKC ζ from TNF-alpha mediated proteolytic cleavage and degradation¹⁰⁹. These findings showed that PKC ζ was cleaved to generate a 50-kDa truncated form with a higher kinase activity than the full length protein¹⁰⁹. As cysts are not subject to fluid flow and TNF-alpha accumulates in cyst fluid¹¹⁰, TNF-alpha signaling could be involved in promoting the cleavage and loss of PKC ζ expression. Interestingly though one of the PKC ζ cleavage fragments has been shown to be constitutively active prior to its rapid degradation¹¹¹. Therefore, it is uncertain whether the reduction of PKC ζ in PKD tissues reflects the loss of PKC ζ signaling or the activation of signaling, perhaps towards different substrates. The precise mechanism by which PKC ζ is downregulated in PKD kidneys remain to be determined.

Our studies show that the reduction of PKC ζ in PKD tissue most likely reflects the loss of normal PKC ζ signaling because pharmacological activation of PKC ζ was found to ameliorate disease progression (Fig. 4, 5). We show that FTY720, an FDA approved drug for

the treatment of multiple sclerosis, upregulates expression of phospho-PKC ζ (Thr⁴¹⁰) *in vitro* and *in vivo*. *In vivo* treatment with FTY720 also strongly reduced markers of disease progression, most notably phospho-STAT3 (Y705) expression. Our findings are in line with a recent report which revealed that FTY720 down regulates STAT3 expression and attenuates inflammatory signaling in cystic Han: SPRD rats¹¹². We expand on their findings to show that when PKC ζ is knocked out, treatment with FTY720 does not relieve the disease to the same degree as in PKC ζ wildtype mice. This effect was observed most significantly when assessing STAT3 activation, which was greatly reduced in PKC ζ wildtype mice treated with FTY720 but was not changed in treated PKC ζ knockout mice. This suggests that FTY720 acts via a PKC ζ dependent mechanism of action to reduce STAT3 over-activation in PKD.

Previous work in our lab reveals that PKC ζ phosphorylates the C-terminal tail of PC1 and that PC1 can regulate STAT3 activity^{6,31}. Because PKC ζ activation also leads to a profound decrease of STAT3 activation in cystic kidneys, it is tempting to speculate that the proposed interaction between PC1 and PKC ζ may also mediate the observed overactivation of STAT3 in ADPKD and numerous mouse models.

Studies indicate that FTY720 becomes phosphorylated by sphingosine kinase 2 (SK2) to produce the active enantiomer (S)-P-FTY720 and acts as a structural analog of Sphingosine-1-phosphate(S1P)¹¹³. Intracellular S1P has been shown to allosterically activate aPKC as a result of direct binding to its kinase domain to relieve autoinhibitory constraints¹¹⁴. By the same logic we can speculate that p-FTY720 binds to and activates PKC ζ . Moreover, studies have shown that FTY720 elevates endogenous levels of ceramide, a well-established activator

of PKC ζ . Ceramide is also critical for the regulation of primarily cilia formation and elongation⁸⁷, a process dysregulated in PKD. FTY720 has also been shown to activate autophagy⁹⁰, which is thought to be suppressed in PKD and to attenuate both fibrosis and inflammation in various animal models of chronic inflammatory diseases^{106,107,116}. Thus, FTY720 provides a very promising therapeutic approach to ADPKD not only by upregulating PKC ζ activity to restore aberrant PKC ζ signaling but also potentially through other mechanisms as well.

Several studies have shown aberrant sphingolipid and glycosphingolipid signaling in ADPKD⁴⁹. Research by Natoli and colleagues reveals that the activation of the mTOR pathway leads to glycosphingolipid (GSL) accumulation and, while the exact mechanism is not known, inhibiting GSL levels slows cyst growth⁵⁰. One possibility may be that by inhibiting glucosyl ceramide (GlcCer) synthase, ceramide metabolism might be driven to favor intracellular sphingosine-1-phosphate biosynthesis and potentially increase PKC ζ activity. Thus, treatment of PKD with GlcCer synthase inhibitors may indirectly affect PKC ζ activation and thereby correct its disrupted expression. If ceramide is more strongly driven toward glucosylceramide formation in PKD the result may be a decreased conversion to intracellular S1P and thus decreased activation of PKC ζ . This serves as another possible explanation for the overall downregulation of PKC ζ activation observed in PKD. Consistent with this notion, a loss of SphK1 which phosphorylates sphingosine to sphingosine-1-phosphate, accelerates cystogenesis¹¹⁷. Although S1P levels have been reported to be increased in polycystic kidneys this may be a reflection of extracellular S1P signaling which regulates pro-inflammatory and pro-survival pathways. Further studies are needed to better understand the complex role of sphingolipid signaling and its influence on PKC ζ expression in PKD.

Loss of PKC ζ levels is commonly observed in cancer and is a prerequisite for the Warburg effect¹¹⁸. Ma and colleagues report that PKC ζ deficiency promotes the metabolic shift necessary for cancer cells to reprogram their metabolism to utilize glutamine in the absence of glucose¹¹⁸. This deficiency enables cancer cells to undergo metabolic reprogramming to help maintain TCA cycle activity and support serine biosynthesis through upregulation of PHGDH. Interestingly, PC1 null cells have also been reported to exhibit features similar to the Warburg effect²⁷. Similar to cancer cells, recent evidence supports that metabolic reprogramming plays a role in proliferation of ADPKD^{27,119}, and our group recently reported that this metabolic inflexibility can be exploited for an effective therapy by inducing the state of ketosis⁵⁴. It is predicted that PKC ζ loss confers a growth advantage in nutrient scarce microenvironments such as cyst lining epithelia. The study by Ma et al. suggests PKC ζ deficiency also results in decreased AMPK activation and autophagy, both pathways which are known to be dysregulated in ADPKD^{57,115}. In fact, AMPK activator Metformin has recently started to be investigated for potential treatment in ADPKD⁶⁰. Therefore, loss of PKC ζ expression in ADPKD cells may be the cause of these related downstream effects.

Altogether, we find that PKC ζ is irregularly expressed in PKD kidneys and can be activated to mitigate disease progression. Our study suggests that FTY720 can stimulate PKC ζ expression resulting in a decrease in activation of disease driver STAT3 as well as in other metrics of PKD. This finding is particularly exciting as FTY720 is already an FDA approved drug. Our results support the potential of FTY720 as a therapeutic for ADPKD and introduces PKC ζ as a pharmacological target for ADPKD therapy.

Material and Methods

Animal Studies. All animal studies were performed in accordance with the rules and regulations of the National Institute of Health with approval of the University of California, Santa Barbara Institutional Animal Care and Use Committee. Mice were maintained in standard vivarium conditions. The bpk/bpk mouse strain was a contribution from Dr. Oliver Wessely at the Cleveland Clinic. The Pkd1^{cond/-} and Pkd1^{cond/cond} mouse models have been described previously^{43,46}. PKC ζ transgenic knockout mice (PKC ζ ^{-/-}) were a contribution from Dr. Jorge Moscat. PKC ζ ^{-/-} mice were crossed into the bpk/bpk and Pkd1^{cond/-} mouse models. All mouse models are on a C57/Bl6 genetic background.

Mice were treated with FTY720 via intraperitoneal (IP) injection every 24 hours. FTY720 (Fingolimod) was obtained from Cayman Chemical Company (Ann Arbor, MI), reconstituted in DMSO and diluted in sterile water to a final concentration of 2% DMSO. Standard injection volume was 10 uL/gram mouse body weight. For the Pkd1^{cond/-}:Nes^{Cre} model, injections were performed from post-natal day 7 to 20. Mice were euthanized on day 21. For the bpk/bpk model, injections were performed from post-natal day 7 to day 16. Mice were euthanized on day 17. Mice were euthanized using a ketamine/xylazine solution, diluted in sterile saline solution. For single injection studies, mice were injected with FTY720 IP and euthanized at the indicated time points following injection. Euthanasia was performed in the same manner.

Mouse Kidney Section Histology and Immunofluorescence Staining. Following euthanasia, kidneys were harvested and longitudinal slices of kidneys were immersion-fixed in 10% neutral buffered formalin for 24 hours, dehydrated in a series of increasing ethanol concentrations and toluene for 2 hours each and imbedded in paraffin wax. 5 μ M sections were cut using a microtome and used for histological and immunofluorescence analysis. All

sections were de-paraffinized in xylene and rehydrated through a series of graded alcohols prior to staining. For immunofluorescence co-staining of aPKC ζ and DBA, deparaffinized sections underwent epitope retrieval by pressure cooking in Tris-EDTA pH 9 (10 mM Tris Base, 1mM EDTA) for 20 minutes, 30 minute incubation in block buffer (5% goat serum, 0.1% TX100 in TBST) at 37°C and incubated in PKC ζ (C24E6) Rabbit mAb (Cell Signaling) (1:200) overnight at 4°C. The next day slides were incubated with Sudan Black B (1% in 70% ethanol) for 20 minutes, washed and incubated in Alexa Fluor 488 Donkey anti-Rabbit IgG (H+L) (ThermoFisher) (1:200) for 1 hour at 37°C. Slides were then washed and incubated in Rhodamine-labeled Dolichos Bioflorus Agglutinin (DBA)(1:100) for one hour at 25°C. For immunofluorescence staining of α -SMA (Abcam) and Ki-67 (Millipore), de-paraffinized 5 μ M sections were subjected to antigen retrieval by pressure-cooking in 10 mM sodium citrate, pH 6. Sections were then incubated in blocking buffer for 60 minutes (1% BSA, 0.1% Triton X-100 and 0.1% gelatin in Tris-Buffered Saline with 0.05% Tween-20; TBST), washed in TBST and incubated at 4 °C overnight in primary antibody diluted 1:200 in blocking buffer. Sections were then incubated in 0.1% Sudan Black B in 70% ethanol for 20 minutes at 25°C to quench auto-fluorescence, washed in TBST and incubated in Alexa Fluor 594 goat anti-rabbit IgG (Invitrogen) (1:1000) in blocking buffer for 1 hour at 37 °C. Immunofluorescence staining of rat anti-mouse F4/80 (Bio-Rad Laboratories) and phospho-STAT3 (Y705) (D3A7) (Abcam) underwent enzymatic epitope retrieval following deparaffinization and were incubated in 20 ug/ml of Proteinase K (Sigma Aldrich) diluted in TE buffer (50mM Tris Base, 1mM EDTA) pH 8 for 20 minutes at 37°C. Phospho-STAT3 stained slides were then blocked in 3% Hydrogen Peroxide (Fisher) in methanol for 30 minutes, blocked in 10% goat serum, 1% BSA, 0.5% Gelatin in Tris-Buffered Saline with

0.05% Tween-20 for an additional 30 minutes at 37 °C and incubated with primary (1:200) overnight at 4°C. Sections were then incubated in Goat anti-Rabbit HRP(Jackson ImmunoResearch) (1:200) for one hour at 25°C, visualized using the DAB-Substrate Kit (Vector Laboratories), dehydrated in increasing grades of ethanol followed by 5 minutes in xylene and mounted with Permount mounting medium (FisherScientific). Following antigen retrieval, slides stained for the macrophage marker F4/80 were blocked in 5% goat serum in TBST for 30 minutes at 37 °C then incubated overnight at 4°C in primary (1:100). Sections were then incubated in 0.1% Sudan Black for 20 minutes at 25°C, washed in TBST and incubated in Alexa Fluor 488 goat anti-rat IgG (Invitrogen) diluted 1:1000 in blocking buffer for 1 hour at 37 °C. Following secondary incubation all fluorescent labeled tissue were washed in TBST, stained with DAPI for 10 minutes at 25 °C and mounted on slides using ProLong Gold Antifade Reagent (Life Technologies). The DeadEnd Fluorometric TUNEL system (Promega) was used for TUNEL staining and performed as specified by the manufacturer.

Cystic Index and Fibrosis Quantification. To quantify the cystic index, tissue sections were stained with hematoxylin and eosin (H&E) and micrographs acquired. Images were overlaid with a grid in Adobe Photoshop and intersecting points on cysts or normal tissue were counted manually. To determine fibrosis, the Sirius Red/Fast Green Collagen Staining Kit was used per assay procedure (#9046, Chondrex, Inc.) and images were obtained for quantification by grid-overlay as described above. Intersecting points on Sirius Red positive areas were counted excluding blood vessels and cysts over the total number of intersections.

Myofibroblast and Macrophage Quantification. To estimate the prevalence of renal myofibroblasts and macrophages, kidney sections were stained for alpha-Smooth muscle actin (SMA) or F4/80 respectively. Grid intersection points on SMA or F4/80 positive structures were counted and divided by the total intersections excluding non-tissue intersections and expressed as a percent.

Ki-67 Quantification. Ki-67 immunostained kidney sections were imaged and the number of cyst lining cells expressing apoptosis marker Ki-67 were counted and expressed as a fraction of the total cyst lining cells. Approximately 1000 cyst-lining cells were counted per kidney section.

TUNEL and Phospho-STAT3 Quantification. TUNEL and pSTAT3-stained sections were imaged and the total number of DAPI-positive nuclei were analyzed using FIJI (ImageJ; NIH) image software. At least 10 areas per kidney were imaged and the number of either TUNEL or pSTAT3 positive cells were counted. Percentages of TUNEL or pSTAT3 positive cells are expressed as a fraction of the total counted nuclei.

Blood Urea Nitrogen (BUN). Blood was extracted via cardiac puncture at the time of euthanasia. Serum was separated using BD Microtainer™ serum separators and frozen. Blood urea nitrogen was quantified using the Urea Nitrogen Colorimetric Detection Kit (Invitrogen, EIABUN) according to the kit procedure.

Cell Culture. Madin-Darby Canine Kidney (MDCK) cells were cultured at 37°C in MEM (Cellgro) supplemented with 5% heat-inactivated fetal bovine serum (Omega Scientific), 1x penicillin/streptomycin (Cellgro) and 1x L-glutamine (Cellgro). Inner medullary collecting duct (IMCD) cells were cultured at 37°C in DMEM F-12 (Cellgro) supplemented with 10%

heat-inactivated fetal bovine serum (Omega Scientific), 1x penicillin/streptomycin (Cellgro) and 1x L-glutamine (Cellgro). Retinal Pigment Epithelial (RPE1) cells were cultured at 37°C in DMEM-RS (Cellgro) supplemented with 4% heat-inactivated fetal bovine serum (Omega Scientific), 1x penicillin/streptomycin and 0.01 mg/mL hygromycin (Thermo/Fisher Scientific).

Immunoblotting. Anti-PKC ζ (C-20), STAT3, STAT3 (Y705) were from Santa Cruz Biotechnology. Anti-actin was from Sigma Aldrich. Anti-aPKC λ was acquired from BD Biosciences. Anti-aPKC ζ/λ (T555/563) was obtained from Invitrogen. Anti-pS6 (Ser240/244), Anti-AMPK, Anti-PKC ζ/λ (T410/403) and Anti-PKC ζ (C24E6) antibodies were acquired from Cell Signaling Technologies. Tissue preparation and loading has been described previously¹²⁰. Briefly, tissues were snap frozen in liquid nitrogen at the time of collection, and then homogenized in a Dounce homogenizer in RIPA lysis buffer. Protein concentrations were estimated using the Promega BCA kit and loaded serially. Each lane represents a single mouse lysate, and lanes between tissues are the same animal for comparison. Bands were quantified using National Institutes of Health (NIH) ImageJ Software.

Human Kidney Samples. Tissue samples from anonymous ADPKD patients or normal controls were obtained from the National Disease Research Interchange (NDRI) as per institutional guidelines. Samples were frozen in liquid nitrogen and then cryo-pulverized using a mortar and pestle. Fine shavings of tissue were lysed in Laemmli sample buffer (lacking bromophenol blue) and were quantified by A280. Normalized samples were used for western blot analysis.

References

1. Wilson, P. D. Polycystic Kidney Disease. *New England Journal of Medicine* **350**, 151–164 (2004).
2. Rangan, G. K. *et al.* Current and emerging treatment options to prevent renal failure due to autosomal dominant polycystic kidney disease. *Expert Opinion on Orphan Drugs* **0**, 1–18 (2020).
3. Weimbs, T. Polycystic kidney disease and renal injury repair: common pathways, fluid flow, and the function of polycystin-1. *Am J Physiol Renal Physiol* **293**, F1423-32 (2007).
4. Antignac, C. *et al.* The future of polycystic kidney disease research—as seen by the 12 Kaplan awardees. *Journal of the American Society of Nephrology* **26**, 2081–2095 (2015).
5. Castelli, M. *et al.* Polycystin-1 binds Par3/aPKC and controls convergent extension during renal tubular morphogenesis. *Nature communications* **4**, 2658 (2013).
6. Doerr, N. E. *Identification of Novel Regulators of Polycystin-1 Signaling*. (University of California, Santa Barbara, 2014).
7. Hughes, J. *et al.* The polycystic kidney disease 1 (PKD1) gene encodes a novel protein with multiple cell recognition domains. *Nat Genet* **10**, 151–60 (1995).
8. Oatley, P., Stewart, A. P., Sandford, R. & Edwardson, J. M. Atomic Force Microscopy Imaging Reveals the Domain Structure of Polycystin-1. *Biochemistry* **51**, 2879–2888 (2012).
9. Sandford, R. *et al.* Comparative Analysis of the Polycystic Kidney Disease 1 (PKD1) Gene Reveals an Integral Membrane Glycoprotein with Multiple Evolutionary Conserved Domains. *Hum Mol Genet* **6**, 1483–1489 (1997).

10. Wilson, P. D. Polycystin: new aspects of structure, function, and regulation. *Journal of the American Society of Nephrology : JASN* **12**, 834–45 (2001).
11. Qian, F. *et al.* Cleavage of polycystin-1 requires the receptor for egg jelly domain and is disrupted by human autosomal-dominant polycystic kidney disease 1-associated mutations. *Proc Natl Acad Sci U S A* **99**, 16981–6 (2002).
12. Parnell, S. C. *et al.* The Polycystic Kidney Disease-1 Protein, Polycystin-1, Binds and Activates Heterotrimeric G-Proteins in Vitro. *Biochemical and Biophysical Research Communications* **251**, 625–631 (1998).
13. Qian, F. *et al.* PKD1 interacts with PKD2 through a probable coiled-coil domain. *Nature genetics* **16**, 179–83 (1997).
14. Chauvet, V. *et al.* Mechanical stimuli induce cleavage and nuclear translocation of the polycystin-1 C terminus. *The Journal of clinical investigation* **114**, 1433–43 (2004).
15. Low, S. H. *et al.* Polycystin-1, STAT6, and P100 function in a pathway that transduces ciliary mechanosensation and is activated in polycystic kidney disease. *Dev Cell* **10**, 57–69 (2006).
16. Li, H. P., Geng, L., Burrow, C. R. & Wilson, P. D. Identification of phosphorylation sites in the PKD1-encoded protein C-terminal domain. *Biochem Biophys Res Commun* **259**, 356–63 (1999).
17. Li, X. *et al.* Protein kinase X (PRKX) can rescue the effects of polycystic kidney disease-1 gene (PKD1) deficiency. *Biochim Biophys Acta* **1782**, 1–9 (2008).
18. Hanaoka, K. *et al.* Co-assembly of polycystin-1 and -2 produces unique cation-permeable currents. *Nature* **408**, 990–4 (2000).

19. Nauli, S. M. *et al.* Polycystins 1 and 2 mediate mechanosensation in the primary cilium of kidney cells. *Nat Genet* **33**, 129–37 (2003).
20. Li, Y., Wright, J. M., Qian, F., Germino, G. G. & Guggino, W. B. Polycystin 2 interacts with type I inositol 1,4,5-trisphosphate receptor to modulate intracellular Ca²⁺ signaling. *J. Biol. Chem.* **280**, 41298–41306 (2005).
21. Woodward, O. M. *et al.* Identification of a polycystin-1 cleavage product, P100, that regulates store operated Ca entry through interactions with STIM1. *PLoS One* **5**, e12305 (2010).
22. Manzati, E. *et al.* The cytoplasmic C-terminus of polycystin-1 increases cell proliferation in kidney epithelial cells through serum-activated and Ca²⁺-dependent pathway(s). *Experimental Cell Research* **304**, 391–406 (2005).
23. Kim, H., Bae, Y., Jeong, W., Ahn, C. & Kang, S. Depletion of PKD1 by an antisense oligodeoxynucleotide induces premature G1/S-phase transition. *European Journal of Human Genetics* **12**, 433–440 (2004).
24. Battini, L. *et al.* Loss of polycystin-1 causes centrosome amplification and genomic instability. *Human Molecular Genetics* **17**, 2819–2833 (2008).
25. Yu, W. *et al.* Identification of polycystin-1 and Gα12 binding regions necessary for regulation of apoptosis. *Cellular Signalling* **23**, 213–221 (2011).
26. Yu, W. *et al.* Polycystin-1 Protein Level Determines Activity of the Gα12/JNK Apoptosis Pathway. *J. Biol. Chem.* **285**, 10243–10251 (2010).
27. Rowe, I. *et al.* Defective glucose metabolism in polycystic kidney disease identifies a new therapeutic strategy. *Nature medicine* **19**, 488–93 (2013).

28. Fischer, E. *et al.* Defective planar cell polarity in polycystic kidney disease. *Nat Genet* **38**, 21–3 (2006).
29. Shillingford, J. M. *et al.* The mTOR pathway is regulated by polycystin-1, and its inhibition reverses renal cystogenesis in polycystic kidney disease. *Proceedings of the National Academy of Sciences of the United States of America* **103**, 5466–71 (2006).
30. Weimbs, T. Regulation of mTOR by polycystin-1: is polycystic kidney disease a case of futile repair? *Cell Cycle* **5**, 2425–9 (2006).
31. Talbot, J. J. *et al.* Polycystin-1 regulates STAT activity by a dual mechanism. *Proc Natl Acad Sci U S A* **108**, 7985–90 (2011).
32. Olsan, E. E. *et al.* Signal transducer and activator of transcription-6 (STAT6) inhibition suppresses renal cyst growth in polycystic kidney disease. *Proceedings of the National Academy of Sciences of the United States of America* **108**, 18067–72 (2011).
33. Talbot, J. J. *et al.* The Cleaved Cytoplasmic Tail of Polycystin-1 Regulates Src-Dependent STAT3 Activation. *Journal of the American Society of Nephrology : JASN* (2014) doi:10.1681/ASN.2013091026.
34. Bhunia, A. K. *et al.* PKD1 Induces p21waf1 and Regulation of the Cell Cycle via Direct Activation of the JAK-STAT Signaling Pathway in a Process Requiring PKD2. *Cell* **109**, 157–168 (2002).
35. Parnell, S. C. *et al.* Polycystin-1 activation of c-Jun N-terminal kinase and AP-1 is mediated by heterotrimeric G proteins. *The Journal of biological chemistry* **277**, 19566–72 (2002).

36. Arnould, T. *et al.* The Polycystic Kidney Disease 1 Gene Product Mediates Protein Kinase C α -dependent and c-Jun N-terminal Kinase-dependent Activation of the Transcription Factor AP-1. *J. Biol. Chem.* **273**, 6013–6018 (1998).
37. Li, X. *et al.* Polycystin-1 and polycystin-2 regulate the cell cycle through the helix–loop–helix inhibitor Id2. *Nature Cell Biology* **7**, 1202–1212 (2005).
38. Puri, S. *et al.* Polycystin-1 activates the calcineurin/NFAT (nuclear factor of activated T-cells) signaling pathway. *J Biol Chem* **279**, 55455–64 (2004).
39. Zhang, B., Tran, U. & Wessely, O. Polycystin 1 loss of function is directly linked to an imbalance in G-protein signaling in the kidney. *Development* **145**, (2018).
40. Dere, R., Wilson, P. D., Sandford, R. N. & Walker, C. L. Carboxy Terminal Tail of Polycystin-1 Regulates Localization of TSC2 to Repress mTOR. *PLoS One* **5**, (2010).
41. Strubl, S. *et al.* STAT signaling in polycystic kidney disease. *Cellular Signalling* **72**, 109639 (2020).
42. Watkins, P. B. *et al.* Clinical Pattern of Tolvaptan-Associated Liver Injury in Subjects with Autosomal Dominant Polycystic Kidney Disease: Analysis of Clinical Trials Database. *Drug Saf* **38**, 1103–1113 (2015).
43. Shillingford, J. M., Piontek, K. B., Germino, G. G. & Weimbs, T. Rapamycin Ameliorates PKD Resulting from Conditional Inactivation of Pkd1. *Journal of the American Society of Nephrology* **21**, 489–497 (2010).
44. Mekahli, D. *et al.* Polycystin-1 but not polycystin-2 deficiency causes upregulation of the mTOR pathway and can be synergistically targeted with rapamycin and metformin. *Pflugers Arch - Eur J Physiol* **466**, 1591–1604 (2014).

45. Ta, M. H. T. *et al.* Effects of TORC1 Inhibition during the Early and Established Phases of Polycystic Kidney Disease. *PLOS ONE* **11**, e0164193 (2016).
46. Kipp, K. R. *et al.* Comparison of folate-conjugated rapamycin versus unconjugated rapamycin in an orthologous mouse model of polycystic kidney disease. *American Journal of Physiology-Renal Physiology* **315**, F395–F405 (2018).
47. Sweeney, W. E., Frost, P. & Avner, E. D. Tesevatinib ameliorates progression of polycystic kidney disease in rodent models of autosomal recessive polycystic kidney disease. *World J Nephrol* **6**, 188–200 (2017).
48. Kadmon Corporation, LLC. *A Double-blind Randomized Parallel Group Study of the Efficacy and Safety of Tesevatinib in Subjects With Autosomal Dominant Polycystic Kidney Disease*. <https://clinicaltrials.gov/ct2/show/NCT03203642> (2020).
49. Natoli, T. A., Modur, V. & Ibraghimov-Beskrovnaya, O. Glycosphingolipid metabolism and polycystic kidney disease. *Cell. Signal.* **69**, 109526 (2020).
50. Natoli, T. A. *et al.* Inhibition of glucosylceramide accumulation results in effective blockade of polycystic kidney disease in mouse models. *Nat Med* **16**, 788–92 (2010).
51. Genzyme, a Sanofi Company. *Multicenter, Randomized, Double-blind, Placebo-controlled Two Stage Study to Characterize the Efficacy, Safety, Tolerability and Pharmacokinetics of GZ/SAR402671 in Patients at Risk of Rapidly Progressive Autosomal Dominant Polycystic Kidney Disease (ADPKD)*. <https://clinicaltrials.gov/ct2/show/NCT03523728> (2020).
52. Sweeney, W. E., von Vigier, R. O., Frost, P. & Avner, E. D. Src Inhibition Ameliorates Polycystic Kidney Disease. *J Am Soc Nephrol* **19**, 1331–1341 (2008).

53. Tesar, V. *et al.* Bosutinib versus Placebo for Autosomal Dominant Polycystic Kidney Disease. *J. Am. Soc. Nephrol.* **28**, 3404–3413 (2017).
54. Torres, J. A. *et al.* Ketosis Ameliorates Renal Cyst Growth in Polycystic Kidney Disease. *Cell Metabolism* **30**, 1007–1023 (2019).
55. Kipp, K. R., Rezaei, M., Lin, L., Dewey, E. C. & Weimbs, T. A mild reduction of food intake slows disease progression in an orthologous mouse model of polycystic kidney disease. *Am J Physiol Renal Physiol* ajprenal 00551 2015 (2016)
doi:10.1152/ajprenal.00551.2015.
56. Torres, V. E. & Harris, P. C. Strategies Targeting cAMP Signaling in the Treatment of Polycystic Kidney Disease. *JASN* **25**, 18–32 (2014).
57. Takiar, V. *et al.* Activating AMP-activated protein kinase (AMPK) slows renal cystogenesis. *Proceedings of the National Academy of Sciences* **108**, 2462–2467 (2011).
58. Shaw, R. J. *et al.* The Kinase LKB1 Mediates Glucose Homeostasis in Liver and Therapeutic Effects of Metformin. *Science* **310**, 1642–1646 (2005).
59. Zhou, G. *et al.* Role of AMP-activated protein kinase in mechanism of metformin action. *J Clin Invest* **108**, 1167–1174 (2001).
60. Seliger, S. L. *et al.* A Randomized Clinical Trial of Metformin to Treat Autosomal Dominant Polycystic Kidney Disease. *AJN* **47**, 352–360 (2018).
61. Chang, M.-Y. *et al.* Metformin Inhibits Cyst Formation in a Zebrafish Model of Polycystin-2 Deficiency. *Scientific Reports* **7**, 7161 (2017).
62. Metformin as a Novel Therapy for Autosomal Dominant Polycystic Kidney Disease - Full Text View - ClinicalTrials.gov. <https://clinicaltrials.gov/ct2/show/NCT02656017>.

63. Zhao, J. *et al.* Low-dose 2-deoxyglucose and metformin synergically inhibit proliferation of human polycystic kidney cells by modulating glucose metabolism. *Cell Death Discovery* **5**, 1–13 (2019).
64. Beebe, J. D., Liu, J.-Y. & Zhang, J.-T. Two decades of research in discovery of anticancer drugs targeting STAT3, how close are we? *Pharmacology & Therapeutics* **191**, 74–91 (2018).
65. Strubl, S. *et al.* STAT signaling in polycystic kidney disease. *Cellular Signalling* 109639 (2020).
66. Takakura, A. *et al.* Pyrimethamine inhibits adult polycystic kidney disease by modulating STAT signaling pathways. *Human molecular genetics* **20**, 4143–54 (2011).
67. Leonhard, W. N. *et al.* Curcumin inhibits cystogenesis by simultaneous interference of multiple signaling pathways: in vivo evidence from a Pkd1-deletion model. *American journal of physiology. Renal physiology* **300**, F1193-202 (2011).
68. Ong, A. C. M. & Harris, P. C. A polycystin-centric view of cyst formation and disease: the polycystins revisited. *Kidney International* **88**, 699–710 (2015).
69. Mochizuki, T. *et al.* PKD2, a gene for polycystic kidney disease that encodes an integral membrane protein. *Science* **272**, 1339–42 (1996).
70. Nauli, S. M. *et al.* Polycystins 1 and 2 mediate mechanosensation in the primary cilium of kidney cells. *Nat Genet* **33**, 129–37 (2003).
71. Yoder, B. K., Hou, X. & Guay-Woodford, L. M. The polycystic kidney disease proteins, polycystin-1, polycystin-2, polaris, and cystin, are co-localized in renal cilia. *Journal of the American Society of Nephrology : JASN* **13**, 2508–16 (2002).

72. Harris, P. C. & Torres, V. E. Polycystic kidney disease. *Annu Rev Med* **60**, 321–37 (2009).
73. Weimbs, T., Olsan, E. E. & Talbot, J. J. Regulation of STATs by polycystin-1 and their role in polycystic kidney disease. *Jak-Stat* **2**, e23650 (2013).
74. Distefano, G. *et al.* Polycystin-1 Regulates Extracellular Signal-Regulated Kinase-Dependent Phosphorylation of Tuberin To Control Cell Size through mTOR and Its Downstream Effectors S6K and 4EBP1. *Molecular and Cellular Biology* **29**, 2359–2371 (2009).
75. Torres, J. A. *et al.* Crystal deposition triggers tubule dilation that accelerates cystogenesis in polycystic kidney disease. *J Clin Invest* **129**, 4506–4522 (2019).
76. Patera, F., Cudzich-Madry, A., Huang, Z. & Fragiadaki, M. Renal expression of JAK2 is high in polycystic kidney disease and its inhibition reduces cystogenesis. *Scientific Reports* **9**, 1–10 (2019).
77. Li, H.-P., Geng, L., Burrow, C. R. & Wilson, P. D. Identification of Phosphorylation Sites in the PKD1-Encoded Protein C-Terminal Domain. *Biochemical and Biophysical Research Communications* **259**, 356–363 (1999).
78. Ohno, S. & Nishizuka, Y. Protein kinase C isotypes and their specific functions: prologue. *Journal of biochemistry* **132**, 509–11 (2002).
79. Moscat, J., Rennert, P. & Diaz-Meco, M. T. PKC ζ at the crossroad of NF- κ B and Jak1/Stat6 signaling pathways. *Cell Death & Differentiation* **13**, 702–711 (2006).
80. Sanz, L., Diaz-Meco, M. T., Nakano, H. & Moscat, J. The atypical PKC-interacting protein p62 channels NF- κ B activation by the IL-1–TRAF6 pathway. *The EMBO Journal* **19**, 1576–1586 (2000).

81. Zhu, H., Moriasi, C. M., Zhang, M., Zhao, Y. & Zou, M.-H. Phosphorylation of Serine 399 in LKB1 Protein Short Form by Protein Kinase C ζ Is Required for Its Nucleocytoplasmic Transport and Consequent AMP-activated Protein Kinase (AMPK) Activation. *J. Biol. Chem.* **288**, 16495–16505 (2013).
82. Hirai, T. Protein Kinase Czeta (PKCzeta): Activation Mechanisms and Cellular Functions. *Journal of Biochemistry* **133**, 1–7 (2003).
83. Joberty, G., Petersen, C., Gao, L. & Macara, I. G. The cell-polarity protein Par6 links Par3 and atypical protein kinase C to Cdc42. *Nat Cell Biol* **2**, 531–9 (2000).
84. Xie, Z., Dong, Y., Scholz, R., Neumann, D. & Zou, M. H. Phosphorylation of LKB1 at serine 428 by protein kinase C-zeta is required for metformin-enhanced activation of the AMP-activated protein kinase in endothelial cells. *Circulation* **117**, 952–62 (2008).
85. Romanelli, A., Martin, K. A., Toker, A. & Blenis, J. p70 S6 Kinase Is Regulated by Protein Kinase C ζ and Participates in a Phosphoinositide 3-Kinase-Regulated Signalling Complex. *Molecular and Cellular Biology* **19**, 2921–2928 (1999).
86. Bourbon, N. A., Yun, J. & Kester, M. Ceramide Directly Activates Protein Kinase C ζ to Regulate a Stress-activated Protein Kinase Signaling Complex. *Journal of Biological Chemistry* **275**, 35617–35623 (2000).
87. Wang, G., Krishnamurthy, K., Umopathy, N. S., Verin, A. D. & Bieberich, E. The carboxyl-terminal domain of atypical protein kinase Czeta binds to ceramide and regulates junction formation in epithelial cells. *J Biol Chem* **284**, 14469–75 (2009).
88. Fox, T. E. *et al.* Ceramide Recruits and Activates Protein Kinase C ζ (PKC ζ) within Structured Membrane Microdomains. *J. Biol. Chem.* **282**, 12450–12457 (2007).

89. Chen, M. B. *et al.* C6 ceramide dramatically increases vincristine sensitivity both in vivo and in vitro, involving AMP-activated protein kinase-p53 signaling. *Carcinogenesis* **36**, 1061–70 (2015).
90. Cruickshanks, N. *et al.* Differential regulation of autophagy and cell viability by ceramide species. *Cancer Biol Ther* **16**, 733–42 (2015).
91. Khazanov, E., Prieve, A., Shillemans, J. P. & Barenholz, Y. Physicochemical and Biological Characterization of Ceramide-Containing Liposomes: Paving the Way to Ceramide Therapeutic Application. *Langmuir* **24**, 6965–6980 (2008).
92. Stover, T. & Kester, M. Liposomal Delivery Enhances Short-Chain Ceramide-Induced Apoptosis of Breast Cancer Cells. *J Pharmacol Exp Ther* **307**, 468–475 (2003).
93. Watters, R. J., Kester, M., Tran, M. A., Loughran, T. P. & Liu, X. Chapter five - Development and Use of Ceramide Nanoliposomes in Cancer. in *Methods in Enzymology* (ed. Düzgüneş, N.) vol. 508 89–108 (Academic Press, 2012).
94. Brinkmann, V. *et al.* Fingolimod (FTY720): discovery and development of an oral drug to treat multiple sclerosis. *Nat Rev Drug Discov* **9**, 883–97 (2010).
95. Lahiri, S. *et al.* Ceramide synthesis is modulated by the sphingosine analog FTY720 via a mixture of uncompetitive and noncompetitive inhibition in an Acyl-CoA chain length-dependent manner. *J Biol Chem* **284**, 16090–8 (2009).
96. Hou, H. *et al.* Fingolimod ameliorates the development of experimental autoimmune encephalomyelitis by inhibiting Akt-mTOR axis in mice. *Int. Immunopharmacol.* **30**, 171–178 (2016).
97. Lu, Z. *et al.* FTY720 inhibits proliferation and epithelial-mesenchymal transition in cholangiocarcinoma by inactivating STAT3 signaling. *BMC Cancer* **14**, 783 (2014).

98. Hait, N. C. *et al.* Active, phosphorylated fingolimod inhibits histone deacetylases and facilitates fear extinction memory. *Nat Neurosci* **17**, 971–80 (2014).
99. Gstalder, C., Ader, I. & Cuvillier, O. FTY720 (Fingolimod) inhibits HIF-1 and HIF-2 signaling, promotes vascular remodeling and chemosensitizes in renal cell carcinoma animal model. *Mol Cancer Ther* (2016) doi:10.1158/1535-7163.MCT-16-0167.
100. Song, C. J., Zimmerman, K. A., Henke, S. J. & Yoder, B. K. Inflammation and Fibrosis in Polycystic Kidney Disease. in *Kidney Development and Disease* (ed. Miller, R. K.) 323–344 (Springer International Publishing, 2017). doi:10.1007/978-3-319-51436-9_12.
101. Norman, J. Fibrosis and progression of Autosomal Dominant Polycystic Kidney Disease (ADPKD). *Biochimica et Biophysica Acta (BBA) - Molecular Basis of Disease* **1812**, 1327–1336 (2011).
102. Cassini, M. F. *et al.* Mcp1 Promotes Macrophage-Dependent Cyst Expansion in Autosomal Dominant Polycystic Kidney Disease. *JASN* **29**, 2471–2481 (2018).
103. Peda, J. D. *et al.* Autocrine IL-10 activation of the STAT3 pathway is required for pathological macrophage differentiation in polycystic kidney disease. *Disease models & mechanisms* **9**, 1051–1061 (2016).
104. Yang, Y. *et al.* Interactions between Macrophages and Cyst-Lining Epithelial Cells Promote Kidney Cyst Growth in Pkd1-Deficient Mice. *JASN* **29**, 2310–2325 (2018).
105. Swenson-Fields, K. I. *et al.* Macrophages promote polycystic kidney disease progression. *Kidney International* **83**, 855–864 (2013).

106. Tian, T. *et al.* FTY720 ameliorates renal fibrosis by simultaneously affecting leucocyte recruitment and TGF- β signalling in fibroblasts. *Clinical & Experimental Immunology* **190**, 68–78 (2017).
107. Ni, H. *et al.* FTY720 prevents progression of renal fibrosis by inhibiting renal microvasculature endothelial dysfunction in a rat model of chronic kidney disease. *J Mol Hist* **44**, 693–703 (2013).
108. Ni, H. F. *et al.* FTY720 attenuates tubulointerstitial inflammation and fibrosis in subtotaly nephrectomized rats. *Ren Fail* **35**, 996–1004 (2013).
109. Garin, G. *et al.* Flow antagonizes TNF- α signaling in endothelial cells by inhibiting caspase-dependent PKC zeta processing. *Circ Res* **101**, 97–105 (2007).
110. Li, X. *et al.* A tumor necrosis factor- α -mediated pathway promoting autosomal dominant polycystic kidney disease. *Nat Med* **14**, 863–8 (2008).
111. Smith, L., Wang, Z. & Smith, J. B. Caspase processing activates atypical protein kinase C zeta by relieving autoinhibition and destabilizes the protein. *The Biochemical journal* **375**, 663–71 (2003).
112. Li, X. *et al.* A Sphingosine-1-Phosphate Modulator Ameliorates Polycystic Kidney Disease in Han:SPRD Rats. *AJN* 1–10 (2019) doi:10.1159/000502855.
113. Billich, A. *et al.* Phosphorylation of the Immunomodulatory Drug FTY720 by Sphingosine Kinases. *J. Biol. Chem.* **278**, 47408–47415 (2003).
114. Kajimoto, T. *et al.* Activation of atypical protein kinase C by sphingosine 1-phosphate revealed by an aPKC-specific activity reporter. *Sci. Signal.* **12**, (2019).
115. Ravichandran, K. & Edelstein, C. L. Polycystic kidney disease: a case of suppressed autophagy? *Seminars in nephrology* **34**, 27–33 (2014).

116. Thangada, S. *et al.* Treatment with the immunomodulator FTY720 (fingolimod) significantly reduces renal inflammation in murine unilateral ureteral obstruction. *J Urol* **191**, 1508–16 (2014).
117. Natoli, T. A. *et al.* Loss of GM3 synthase gene, but not sphingosine kinase 1, is protective against murine nephronophthisis-related polycystic kidney disease. *Hum Mol Genet* **21**, 3397–407 (2012).
118. Ma, L. *et al.* Control of nutrient stress-induced metabolic reprogramming by PKCzeta in tumorigenesis. *Cell* **152**, 599–611 (2013).
119. Podrini, C. *et al.* Dissection of metabolic reprogramming in polycystic kidney disease reveals coordinated rewiring of bioenergetic pathways. *Communications Biology* **1**, (2018).
120. Kipp, K. R., Rezaei, M., Lin, L., Dewey, E. C. & Weimbs, T. A mild reduction of food intake slows disease progression in an orthologous mouse model of polycystic kidney disease. *American Journal of Physiology - Renal Physiology* **310**, F726–F731 (2016).